Role of Phosphatidylinositol 3′ Kinase and a Downstream Pleckstrin Homology Domain–containing Protein in Controlling Chemotaxis in *Dictyostelium*

Satoru Funamoto, Kristina Milan, Ruedi Meili, and Richard A. Firtel

Section of Cell and Developmental Biology and Center for Molecular Genetics, University of California at San Diego, La Jolla, California 92093

Abstract. We show that cells lacking two *Dictyostelium* class I phosphatidylinositol (PI) 3′ kinases (PI3K and *pi3k1/2*-null cells) or wild-type cells treated with the PI3K inhibitor LY294002 are unable to properly polarize, are very defective in the temporal, spatial, and quantitative regulation of chemoattractant-mediated filamentous (F)-actin polymerization, and chemotax very slowly. PI3K is thought to produce membrane lipid-binding sites for localization of PH domain–containing proteins. We demonstrate that in response to chemoattractants three PH domain–containing proteins do not localize to the leading edge in *pi3k1/2*-null cells, and the translocation is blocked in wild-type cells by LY294002. Cells lacking one of these proteins, *phdA*-null cells, exhibit defects in the level and kinetics of actin polymerization at the leading edge and have chemotaxis phenotypes that are distinct from those described previously for protein kinase B (PKB) (*pkbA*)-null cells. Phenotypes of PhdA-dominant interfering mutations suggest that PhdA is an adaptor protein that regulates F-actin localization in response to chemoattractants and links PI3K to the control of F-actin polymerization at the leading edge during pseudopod formation. We suggest that PKB and PhdA lie downstream from PI3K and control different downstream effector pathways that are essential for proper chemotaxis.

Key words: *Dictyostelium* • PH domain • actin polymerization • chemotaxis • PI3 kinase

Introduction

Phosphatidylinositol (PI)[1] 3′ kinase (PI3K) is a regulator of cell growth and survival in higher eukaryotes (Leevers et al., 1999; Rameh and Cantley, 1999; Vanhaesebroeck and Waterfield, 1999). Activation of PI3K produces the membrane-soluble products PI 3,4,5-triphosphate (PI[3,4,5]P_3) and PI 3,4-bisphosphate (PI[3,4]P_2), resulting in the membrane localization and activation of downstream effectors. In mammalian cells, the PI3K effector protein kinase B ([PKB] or Akt) inhibits apoptosis, regulates GSK3 and cell metabolism, and posttranscriptionally regulates gene expression (Cross et al., 1995; Datta et al., 1997; Cardone et al., 1998; Brunet et al., 1999; Gold et al., 1999; Kennedy et al., 1999; Osada et al., 1999; Tang et al., 1999). In *Caenorhabditis elegans*, PI3K and PKB control dauer larval formation; in *Drosophila*, PI3K regulates cell size (Paradis and Ruvkun, 1998; Weinkove et al., 1999). Furthermore, PI3Kγ regulates chemotaxis in different classes of leukocytes (Dunzendorfer et al., 1998; Vanhaesebroeck et al., 1999; Hirsch et al., 2000; Li et al., 2000; Sasaki et al., 2000).

Dictyostelium contains three class I PI3Ks (Zhou et al., 1995). Two, PI3K1 and PI3K2, are genetically redundant and most closely related to the mammalian class I_A PI3K p110α (Vanhaesbroeck et al., 1997). The third, PI3K3, is most closely related to PI3Kγ. (The *Dictyostelium* PI3Ks were originally called DdPI3K1, DdPI3K2, and DdPI3K3 [Zhou et al., 1995], but the names were shortened to PI3K1, PI3K2, and PI3K3 [Meili et al., 1999, 2000].) Disruption of *PI3K1* and *PI3K2* (*pi3k1/2*-null cells, previously called *Δddpi3k1/pi3k2*) results in cells that are small, grow slowly (Zhou et al., 1995), have an aberrant cell structure, are poorly polarized, and are defective in endocytosis (Buczynski et al., 1997). In addition, these cells exhibit an aggregation defect that suggests they do not chemotax effectively (Zhou et al., 1998), which is consistent with the requirement of PI3Kγ for chemotaxis in mammalian cells (Dunzendorfer et al., 1998; Vanhaesebroeck et al., 1999; Hirsch et al., 2000; Li et al., 2000; Sasaki et al., 2000) but in conflict with results reported previously by Buczynski et al. (1997). Disruption of *Dictyostelium* PI3K3 has no ob-

Address correspondence to Richard A. Firtel, Center for Molecular Genetics, Rm. 225, University of California at San Diego, 9500 Gilman Dr., La Jolla, CA 92093-0634. Tel.: (858) 534-2788. Fax: (858) 534-7073. E-mail: rafirtel@ucsd.edu

[1]*Abbreviations used in this paper:* CRAC, Ca^{2+} release-activated Ca^{2+}; GFP, green fluorescent protein; PH, pleckstrin homology; PhdA, PH domain–containing protein A; PI, phosphatidylinositol; PI3K, PI 3′-kinase; PI (3,4,5)P_3, PI 3,4,5-triphosphate; PI (3,4)P_2, PI 3,4-bisphosphate; PKB, protein kinase B.

servable phenotype, although studies suggest that a double knockout of PI3K3 with either PI3K1 or PI3K2 is lethal (Zhou et al., 1995), implying that basal PI3K activity is essential for cell growth in *Dictyostelium*.

Studies on *Dictyostelium* PKB, a PI3K effector, suggest PI3K function is required for cell polarity and proper chemotaxis (Meili et al., 1999, 2000). *Dictyostelium* PKB is rapidly and transiently activated in response to chemoattractants via a receptor-mediated, PI3K–dependent pathway. When placed in a chemoattractant gradient, *pkbA*-null cells do not polarize and move very slowly. Although wild-type cells produce pseudopodia almost exclusively from the leading edge, *pkbA*-null cells produce multiple pseudopodia simultaneously in all directions. The PKB PH domain rapidly and transiently translocates to the plasma membrane upon chemoattractant stimulation and is found at the leading edge in chemotaxing cells. The kinetics of membrane translocation and kinase activity suggest a causal relationship between membrane localization of PKB and its activation (Meili et al., 1999) and are consistent with results in mammalian cells (Andjelkovic et al., 1997). Chemoattractants stimulate PKB activity in mammalian cells (Tilton et al., 1997), and the pleckstrin homology (PH) domain of mammalian PKB exhibits a similar chemoattractant-regulated membrane localization in neutrophils (Servant et al., 2000). These results suggest that these basic mechanisms are conserved between mammalian and *Dictyostelium* cells and that PKB may be a key regulator of cell polarity and chemotaxis in leukocytes. PI3K1 and PI3K2 are required for PKB activation, indicating PI3K is required for chemotaxis in *Dictyostelium*, and results suggesting *pi3k1/2*-null cells chemotax more rapidly than wild-type cells are incorrect (Buczynski et al., 1997).

The analyses of several PH domain–containing proteins in *Dictyostelium* and mammalian cells indicate a broad role for PI3K in regulating localized responses at the leading edge of chemotaxing cells (Parent et al., 1998; Meili et al., 1999; Servant et al., 2000). We and others have proposed that a localized activation of PI3K at the leading edge leads to the formation of PI(3,4,5)P_3- and PI(3,4)P_2-enriched lipid domains that function as docking sites for diverse PH domain–containing proteins, resulting in an enrichment of these proteins, localized responses, the formation of a new pseudopod, and directed cell movement (Parent and Devreotes, 1999; Firtel and Chung, 2000; Rickert et al., 2000). Here, we characterize the role of PI3K in chemotaxis through a detailed analysis of the phenotypes of *pi3k1/2*-null cells, wild-type cells treated with the PI3K inhibitor LY294002, and a new PI3K effector. Our findings support the model presented above for PI3K function and provide a new linkage between PI3K, actin polymerization, and chemotaxis that is independent of the activation of PKB.

Materials and Methods

Cell Culture and Development

Dictyostelium cells, strain KAx-3, were grown in axenic HL5 medium and transformed by electroporation. For gene disruptions, we selected cells in the presence of blasticidin. We observed morphology by plating washed exponentially growing cells on nonnutrient agar plates (Ma et al., 1997).

Because of concerns about the original *pi3k1/2*-null strain, we remade the strain in the KAx-3 background. It is designated GMP1.

Constructs

We generated a *phdA* knockout construct by inserting the blasticidin resistance cassette into the XbaI and BamHI sites of a PH domain–containing protein A (PhdA) ORF inserted in pSP72. For PhdA–green fluorescent protein (GFP) fusion protein expression, PhdA was amplified by PCR, ligated to a GFP fragment, and cloned into the expression vector EXP-4(+). A mutant, $PhdA^{R41C}$, was generated using PCR. Successful mutagenesis was confirmed by sequencing.

Chemotaxis and Image Acquisition

The analyses of chemotaxis towards cAMP and global responses to cAMP were done as described previously (Chung and Firtel, 1999) and analyzed with the DIAS program (Soll and Voss, 1998). We performed folate chemotaxis on starved cells grown in association with *Klebsiella aerogenes* using a Dunn chamber with 5 μM folate.

Quantitation of membrane or cortical localization of GFP fusion of PH domain–containing proteins and GFP-coronin in wild-type cells represents the averages of at least five cells from at least three separate experiments. We measured the intensity of cortical GFP by line scanning with Metamorph software. The level of cortical GFP was calculated by dividing intensity before stimulation (E_0) by intensity at each time point (E) after subtraction of basal intensity (Moniakis et al., 2001).

We added LY294002 to a final concentration of 30 μM 10 min before the addition of cAMP for biochemical assays, real time recording of chemotaxis toward the micropipette or translocation of GFP fusion proteins. No differences were observed if the drug was added either 30 or 60 min before stimulation.

Biochemical Assays

We measured the amount of F-actin in response to cAMP stimulation using TRITC phalloidin as described (Chung et al., 2000). The values are the averages of at least three separate experiments. We assayed guanylyl cyclase using the cGMP assay kit (Amersham Pharmacia Biotech) (Ma et al., 1997). PKB activity was measured as described (Meili et al., 1999). Adenylyl cyclase was measured by C. Parent (Parent and Devreotes, 1995).

To measure the in vitro translocation of PhdA, cells expressing PhdA–GFP were pulsed with cAMP and treated with caffeine as described previously (Chung et al., 2000), resuspended at 8×10^7 cells/ml in 5 mM $NaPO_4$ buffer containing 2 mM $MgSO_4$, and filter lysed using Nuclepore filters in the presence or absence of 40 μM GTPγS and 1 μM cAMP. We incubated the cell lysates for 5 min on ice. To stop the reaction, we added 1 ml of ice-cold phosphate buffer. Membrane fractions were collected by centrifugation for 1 min at 15,000 *g* and subjected to immunological detection of PhdA–GFP by using anti-GFP antibody (BABCO). In separate experiments, the cells were lysed in the presence of 40 μM GDPβS or in the presence of 40 μM GTPγS and 12.5 μM LY294002.

Results

pi3k1/2-null Cells Exhibit Aberrant Chemotaxis

The analyses by Zhou et al. (1998) on *pi3k1/2*-null cells and Meili et al. (1999, 2000) on *pkbA*-null cells suggest that PI3K is required for proper cell polarity and chemotaxis. Since these results conflict with previously published results on *pi3k1/2*-null cells, which suggest that *pi3k1/2* cell chemotax more rapidly than wild-type cells (Buczynski et al., 1997), we have undertaken a detailed analysis of chemotaxis of *pi3k1/2*-null cells using more current experimental technologies and analysis methods.

Fig. 1 shows an analysis of the ability of *pi3k1/2*-null cells (strain GMP1; see Materials and Methods) to chemotax towards a micropipette containing the chemoattractant cAMP. These cells are poorly polarized (not elongated) and move very slowly compared with wild-type cells, as illustrated by the number of cells that

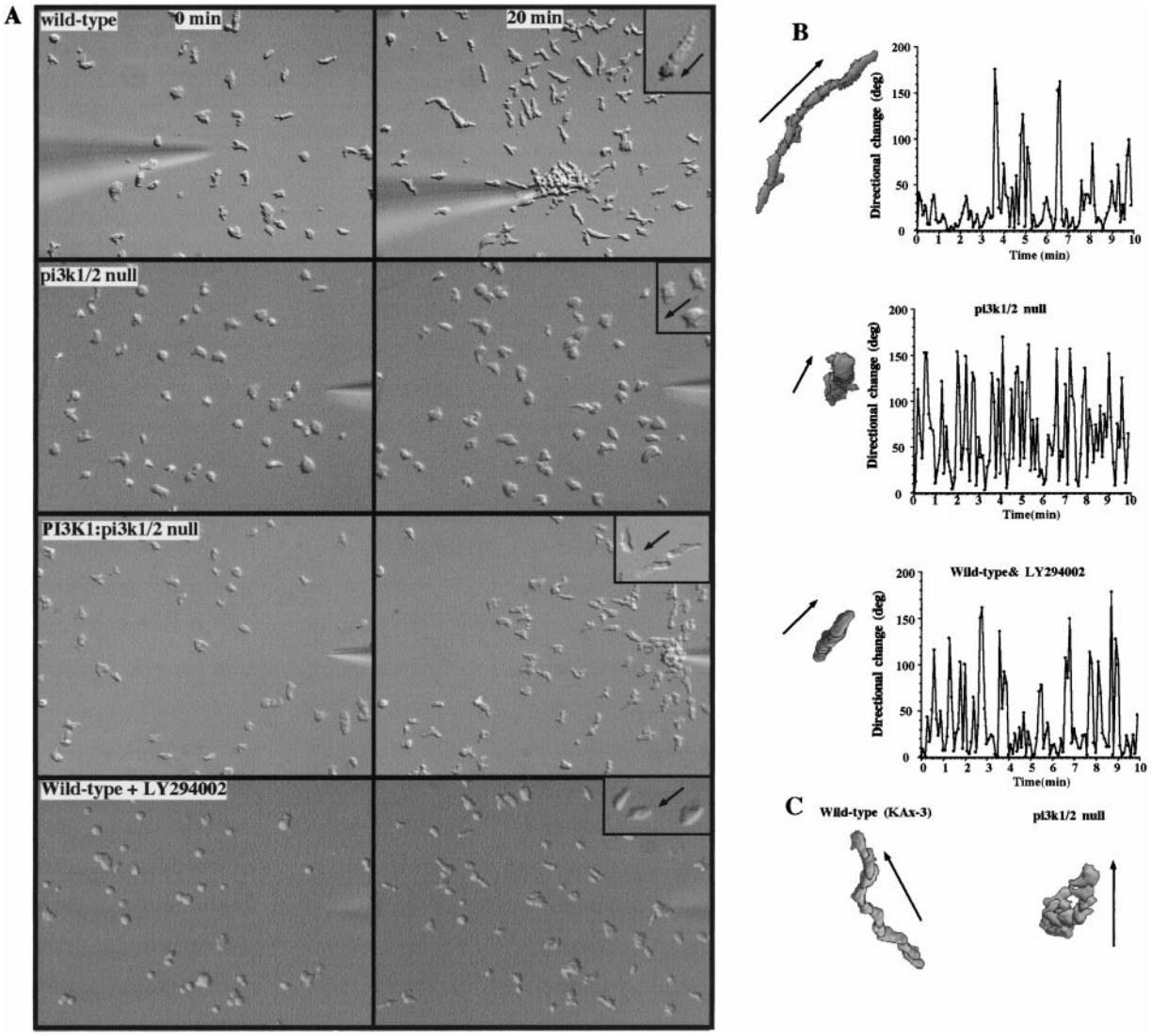

Figure 1. Time-lapse recording of chemotaxis of wild-type and *pi3k1/2*-null cells. (A) After pulsing with cAMP, cells were transferred to glass-bottomed dishes and allowed to adhere to the bottom. A needle filled with 150 μM cAMP was placed on the bottom and is visible in the images. The movement of wild-type cells, *pi3k1/2*-null cells, *pi3k1/2*-null cells expressing PI3K1, or wild-type cells plus 30 μM LY294002 toward the cAMP source was recorded (Chung and Firtel, 1999). Zero- (0; when the micropipette was inserted) and 20-min time points are shown. The insets show an enlargement of representative cell(s). (B) DIAS computer analyses. See Table I for the numerical analysis. (C) Chemotaxis to folate in a Dunn chamber. Superimposed images at 1-min intervals depict the movement of these strains and give an indication of the chemotaxis efficiency. The graphs plot the change of direction ofthe leading edge relative to the cell's centroid.

move toward the micropipette tip over a period of time. This phenotype is similar to that of *pkbA*-null cells and consistent with the conclusion that PKB lies downstream from PI3K (Meili et al., 1999). We quantitated the chemotaxis parameters of the *pi3k1/2*-null cells, including cell shape and directionality of cell movement (an indicator of chemotaxis efficiency), using the DIAS computer software program (Soll and Voss, 1998). This analysis indicates that *pi3k1/2-null* cells are more rounded and move more slowly than wild-type cells and produce pseudopodia randomly along the sides of the cells rather than predominantly at the leading edge, as do wild-type cells (Fig. 1 and Table I). As a result, the cells chemotax very inefficiently with low directionality (Table I). Expression of PI3K in *pi3k1/2*-null cells complements the growth and developmental phenotypes of this strain (Zhou et al., 1995).

Since the ability of cells to respond to extracellular cAMP is developmentally regulated, we wanted to ensure these cells were competent to respond to extracellular cAMP. RNA blot analysis revealed that the level of expression of the cAMP receptor cAR1 in response to pulses of cAMP was only slightly lower than that of wild-type cells and well within the range of other responsive cell types (data not shown). *Dictyostelium* has a PKB and a related kinase, PKBR-1, that differs from PKB in that it lacks a PH domain and is constitutively membrane localized via myristoylation (Meili et al., 2000). Like PKB, PKBR-1 kinase activity is stimulated in response to cAMP; however, unlike the activation of PKB the activa-

Table I. DIAS Analysis of Chemotaxis

Strain	Speed*	Direction of change‡	Roundness§	Directionality‖
	μm/min	*degree*	*%*	
Wild-type (KAx-3)	9.2 ± 1.60	30.2 ± 4.4	43.3 ± 4.8	0.74 ± 0.05
pi3k1/2-null	4.1 ± 0.89	59.3 ± 9.3	70.2 ± 4.5	0.29 ± 0.17
PI3K1:*pi3k1/2*-null	9.3 ± 0.92	28.4 ± 5.7	43.2 ± 4.6	0.73 ± 0.03
phdA-null	3.5 ± 0.60	61.6 ± 8.6	54.1 ± 2.9	0.32 ± 0.08
PhdA/*phdA*-null	8.0 ± 1.50	35.6 ± 9.1	37.3 ± 1.8	0.70 ± 0.09
PhdA/KAx-3	8.20 ± 1.60	30.1 ± 6.3	48.9 ± 3.6	0.73 ± 0.07
$PhdA^{R41C}$/KAx-3	5.74 ± 1.04	40.4 ± 6.8	53.3 ± 10.0	0.59 ± 0.11
Wild-type + LY294002	5.0 ± 0.88	36.6 ± 4.0	74.5 ± 1.8	0.60 ± 0.01
pi3k1/2-null + LY294002	4.0 ± 0.33	40.4 ± 2.5	69.3 ± 5.8	0.57 ± 0.04
PKB overexpressor	8.1 ± 1.2	37.5 ± 7.0	45.0 ± 5.4	0.66 ± 0.13

DIAS computer analysis was performed from digital time-lapse video differential interference contrast microscopy movies of the listed strains chemotaxing to cAMP. A 40× objective was used for the movies.
*Indicates speed of movement of the cell's centroid and not the actual distance traveled over a specified time.
‡Changes in direction (in degrees) is a relative measure of the number and frequency of turns the cell makes. The parameter measures the change (in degrees) in the position of the new pseudopod (leading edge) relative to the position of the cell's centroid. Higher numbers indicate more turns and less efficient chemotaxis.
§Roundness is an indication of the polarity of the cells. Larger numbers indicate the cells are more round and less polarized.
‖Directionality is a measure of how straight the cells move. Cells moving in a straight line have a directionality of 1.0.

tion of PKBR-1 is not inhibited by the PI3K inhibitor LY294002 (Meili et al., 2000). We found that PKBR-1 activation is normal in both the level of kinase activity and its kinetics in *pi3k1/2*-null cells, indicating that *pi3k1/2*-null cells exhibit some normal cAMP-mediated responses and the cells are not generally unresponsive.

To support our conclusions that PI3K plays a key role in chemotaxis and to eliminate possible concerns that *pi3k1/2*-null cells may be less developmentally competent to respond to the chemoattractant cAMP, we examined the effect of treatment of aggregation-stage cAMP-responsive wild-type cells with the PI3K inhibitor LY294002 on chemotaxis. For these experiments, we used a concentration of 30 μM of the drug, which we demonstrate to be the lowest concentration that effectively inhibits translocation of PH domains to the plasma membrane in response to chemoattractant stimulation and PKB activation (Meili et al., 1999, 2000; see below, Fig. 4 C) (note, this concentration varies with the lot of LY294002). As shown in Fig. 1 and Table I, these cells have polarity and chemotaxis defects similar to those of *pi3k1/2*-null cells. One noticeable difference is that LY294002-treated wild-type cells display fewer changes in the direction of cell movement than *pi3k1/2*-null cells and, for the most part, are more rounded and produce fewer pseudopodia. This difference may be due to the level of inhibition of the PI3K pathways by the drug, which presumably inhibits all three PI3Ks (Meili et al., 1999, 2000). To test this possibility, we examined the chemotaxis behavior of *pi3k1/2*-null cells treated with LY294002. These cells exhibited phenotypes more severe than those of *pi3k1/2*-null cells and similar to those of LY294002-treated wild-type cells (Table I).

Dictyostelium cells also chemotax to folic acid, a response that is maximal shortly after starvation in cells grown on bacteria (Varnum and Soll, 1981). However, the chemotaxis response is not as robust as that to cAMP during the aggregation stage, and the response is maximal at much higher concentrations of ligand (1–10 μM). Because of this, cells do not chemotaxis effectively to folate emitted from a micropipette, possibly because of the inability to establish an appropriate chemoattractant gradient, but they do chemotax effectively to folate in a Dunn chamber (Insall, R., personal communication). Analysis of bacterially grown wild-type and *pi3k1/2*-null cells revealed that wild-type cells chemotax with a directionality of 0.84 ± 0.05, whereas *pi3k1/2*-null cells chemotax with a directionality of only 0.38 ± 0.18 (Fig. 1 C). The results demonstrate definitively that *pi3k1/2*-null cells exhibit chemotaxis defects to two chemoattractants at different stages of development. These results expand on those of Zhou et al. (1998) but disagree with those of Buczynski et al. (1997); the reason for the discrepancy between the present and previous findings on *pi3k1/2*-null cells is unknown.

pi3k1/2-null Cells Exhibit Defects in Chemoattractant-mediated Actin Polymerization

When cells are rapidly bathed in the chemoattractant cAMP, which simultaneously activates all receptors on the cell surface, wild-type *Dictyostelium* cells exhibit a transient ~2.2-fold increase in the level of F-actin that peaks ~5 s after cAMP addition (Carboni and Condeelis, 1985; Condeelis and Hall, 1991). *pi3k1/2*-null cells exhibit a reduced basal level of F-actin (zero time point), and the chemoattractant-mediated F-actin assembly is reduced significantly compared with that of wild-type cells (Fig. 2 A).

Figure 2. Changes in F-actin in *pi3k1/2*-null cells in response to chemoattractant stimulation. (A) F-actin levels in wild-type, *pi3k1/2*-null cells, and wild-type cells plus 30 μM LY294002 after cAMP stimulation. The F-actin content was determined as described previously (Chung et al., 2000). (Wild-type cells treated with 10 μM LY294002 showed little effect on changes in F-actin; 30 and 60 μM had similar effects; 90 μM had a slightly greater effect [see Fig. 4 C; data not shown].) (Ba) Cells expressing GFP-coronin were globally stimulated with saturating (μM) levels of cAMP. Changes in the localization of GFP-coronin, as determined by fluorescence, were followed as described in Materials and Methods. (Wild-type cells treated for 10 min with LY294002 are round in the absence of a cAMP gradient.) (Bb) Kinetics of GFP-coronin translocation to the membrane after cAMP stimulation. Intensity of fluorescence on the membrane was measured using Metamorph software. Graph shows increase fold calculated by dividing intensity before stimulation (E_0) by intensity at each time

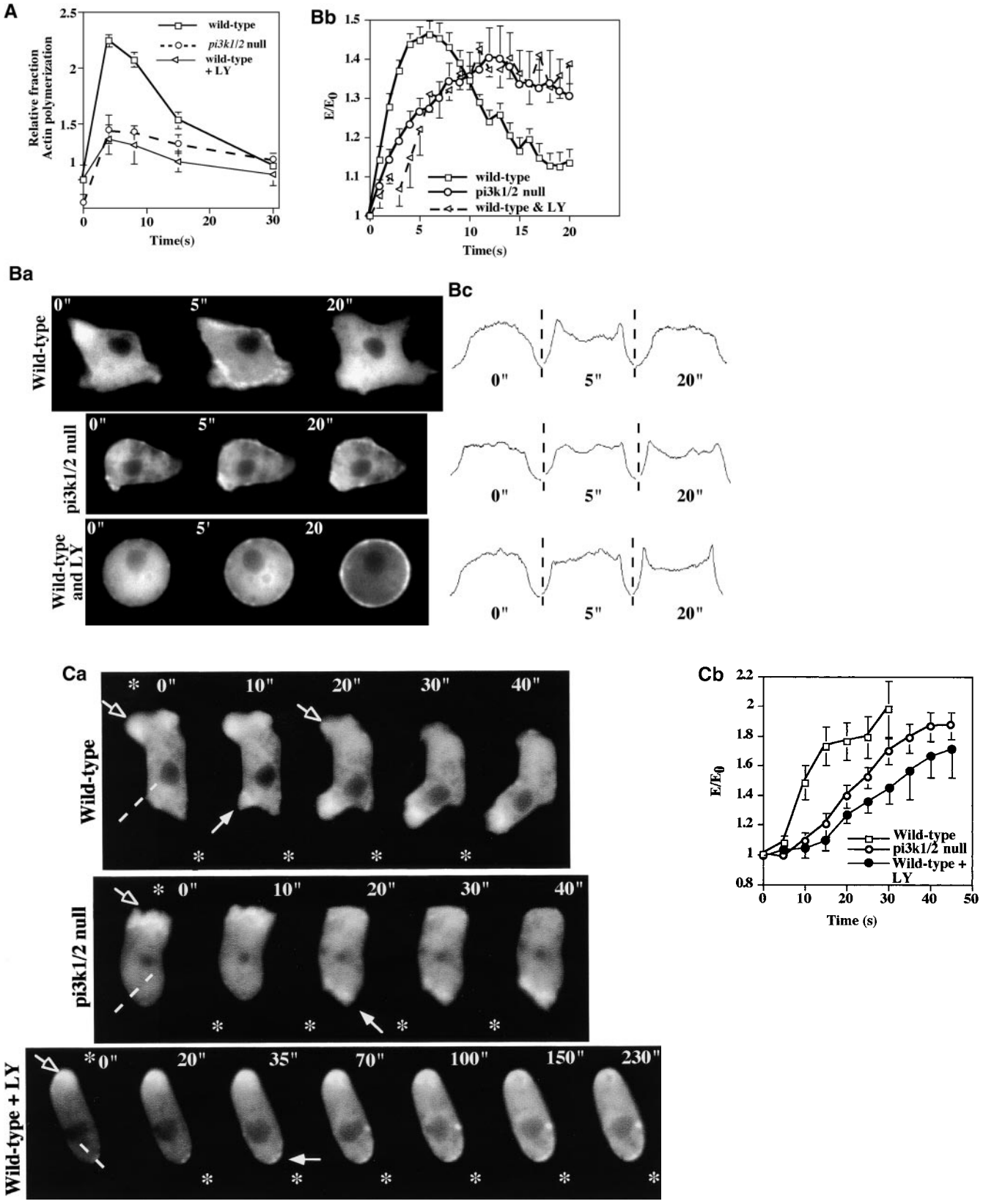

point (E). (Bc) Intensity profiles of images in Ba. (Ca) Translocation of coronin in response to changes in the position of the micropipette containing cAMP. Placing the tip of a micropipette filled with 150 μM cAMP near the cell causes the accumulation of GFP-coronin at the edge of the cell closest to the tip and the formation of a new pseudopod. Changing the position of the tip to the opposite side results in the formation of new pseudopodia enriched in GFP-coronin and a retraction of the old pseudopod. Asterisks indicate the position of the micropipette. Open arrow indicates retracting pseudopod; white arrow indicates new pseudopod. (Cb) Kinetics of translocation of coronin. The graph shows fold increase calculated by dividing intensity before stimulation (E_0) by intensity at each time point (E).

The level of F-actin stays elevated for a longer period of time, ≥30 s after stimulation, whereas the level of F-actin in wild-type cells returns to prestimulation levels in that time. Wild-type cells pretreated with LY294002 display a pattern and level of cAMP-stimulated F-actin similar to those of *pi3k1/2*-null cells but with a higher basal level of F-actin (Fig. 2 A). The dose–response curve of LY294002 inhibition of F-actin assembly is very similar to that of PH domain translocation (data not shown; see Fig. 4 C).

Although these experiments quantitate F-actin polymerization in response to global stimulation, they do not provide an accurate measurement of the kinetics of new F-actin polymerization during pseudopod formation or the ability of cells to spatially respond to changes in the direction of a chemoattractant gradient. Such changes can be dynamically visualized in chemotaxing cells using a GFP fusion of the F-actin–binding protein coronin (Gerisch et al., 1995). When wild-type cells expressing GFP-coronin are given a global stimulation, GFP-coronin becomes uniformly localized to the cell cortex (Fig. 2 Ba), as expected from the analysis of F-actin localization and previous results using this reporter (Gerisch et al., 1995). We quantitated the kinetics of this response by measuring the increase in fluorescence across the plasma membrane. In wild-type cells, GFP-coronin translocation peaks at ~5 s, similar to the kinetics of F-actin assembly measured biochemically (Fig. 2 Bb). In contrast, the increase is reduced in *pi3k1/2*-null cells (cells expressed GFP-coronin at a similar level as determined by the fluorescence of unstimulated cells) and the kinetics are extended (Fig. 2 Bb), similar to our observations in the actin polymerization assays. Wild-type cells treated for 10 min with LY294002 become very rounded, exhibiting a loss of polarity (Chung et al., 2001). When stimulated with cAMP, these cells show kinetics of cortical GFP-coronin that are very similar to those of *pi3k1/2*-null cells, consistent with PI3K being required for this process.

To study the ability of cells to form a new pseudopod, we placed GFP-coronin–expressing cells in a chemoattractant gradient and examined the subcellular localization of the fluorescent signal as the cells moved towards the micropipette. As demonstrated previously, GFP-coronin localizes to the cortex of the leading edge in wild-type cells (Gerisch et al., 1995; Fig. 2 C). When we move the micropipette to a new position relative to the cell, the old pseudopod rapidly retracts and a new one forms proximal to the new cAMP source with a half-maximal response at ~10 s. With the retraction of the old pseudopod, there is a concomitant loss of GFP-coronin from this site on the cell and an enrichment of GFP-coronin at the position of the new pseudopod (Gerisch et al., 1995). Phalloidin staining indicates that the GFP-coronin signal colocalizes with F-actin formation (data not shown). In *pi3k1/2*-null cells, the kinetics of the formation of a new pseudopod and the loss of the old pseudopod were also delayed, with the half-maximal response for the formation of the new pseudopod occurring at ~24 s and a delay in the initial response (Fig. 2 C). In addition, the kinetics of the loss of the old pseudopod, as determined by the loss of GFP-coronin signal, were significantly slower in *pi3k1/2*-null cells. This aspect of the phenotype cannot be readily quantified but is observable by examining the intensity of fluorescence in time-lapse pictures (Fig. 2 C). Similar experiments in LY294002-treated wild-type cells showed a very delayed response that exhibited a much greater cell-to-cell variability in the kinetics (Fig. 2 C). These results are consistent with a requirement for PI3K in the proper spatiotemporal regulation of F-actin localization in response to chemoattractants.

Identification of the Gene Encoding PhdA, a New PH Domain–containing Protein Required for Aggregation

As the growth and aggregation phenotypes of the *pi3k1/2*-null cells are more severe than those of PKB (*pkbA*)-null cells, we expect that other PI3K effectors were required for chemotaxis in addition to PKB. As in the model outlined in the Introduction, such proteins might contain a PH domain.

A new gene, *PhdA*, was identified in a genetic screen for mutant strains with developmental defects (strain DG1093; http://www-biology.ucsd.edu/others/dsmith/REMIgenes2000.html). The developmental phenotype suggested that *phdA*-null cells exhibit aggregation and, potentially, chemotaxis defects. An independently derived *phdA*-null strain was created by homologous recombination and used for the described experiments (see Materials and Methods). When plated for development, *phdA*-null cells form very small aggregates and fruiting bodies similar to the phenotype of *mek1-null* cells, which are defective in chemotaxis (Ma et al., 1997). The *phdA*-null strain developmental phenotypes are complemented by expressing PhdA or a PhdA–GFP fusion protein from the constitutive *Actin 15* promoter (Fig. 3 A; data not shown).

The derived PhdA ORF encodes a 284–amino acid protein with an NH_2-terminal PH domain and a short novel COOH-terminal domain (Fig. 3 C; sequence data available from GenBank/EMBL/DDBJ under accession no. AF080677). The PH domain shares homology with the PH domains of PKB and Ca^{2+} release-activated Ca^{2+} (CRAC), a cytoplasmic protein required for receptor-mediated adenylyl cyclase activation in *Dictyostelium* (Insall et al., 1994). BLAST analysis indicates that the PhdA COOH terminus is novel, but very weak homology is observed in a one-to-one comparison with the COOH terminus of CRAC, suggesting that PhdA and CRAC may be distantly related. PhdA expresses two distinct transcripts, a larger one expressed during growth and early development and a smaller transcript induced during mound formation (Fig. 3 B).

PhdA Translocates to the Leading Edge via a PI3K–dependent Pathway

The presence of a PH domain related to those in PKB and CRAC suggests that PhdA may also translocate to the plasma membrane in response to a global stimulation by cAMP and to the leading edge in chemotaxing cells. To examine this, we used a PhdA–GFP fusion protein and performed time-lapse videomicroscopy.

In unstimulated cells, PhdA–GFP exhibits a uniform distribution throughout the cell. In response to global stimulation, there is a rapid and transient translocation of PhdA–GFP from the cytosol to the plasma membrane,

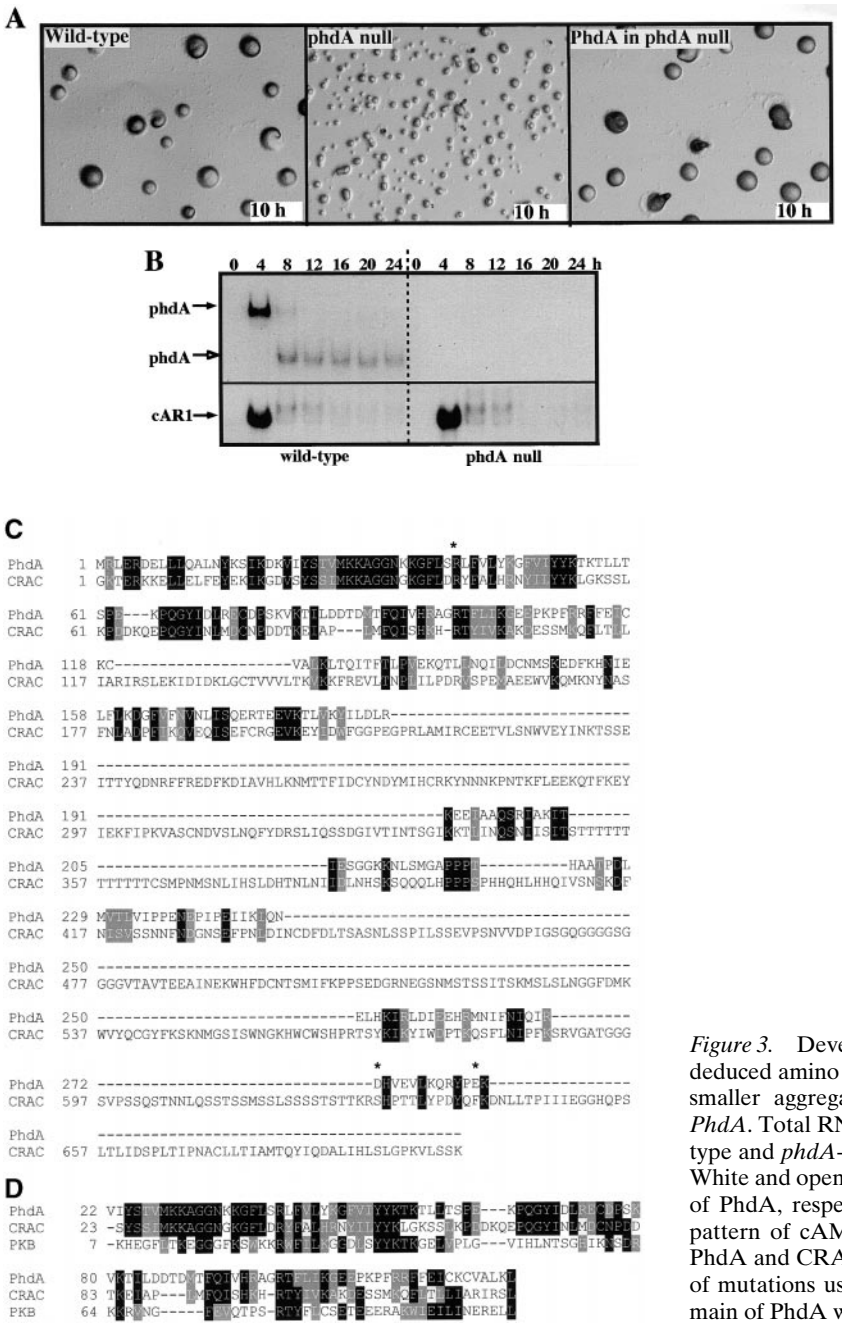

Figure 3. Development morphology of *PhdA* mutant strains and deduced amino acid sequence of PhdA. (A) *phdA*-null cells form smaller aggregates. (B) Developmental expression pattern of *PhdA*. Total RNAs were isolated at the time indicated from wild-type and *phdA*-null cells and subjected to Northern blot analysis. White and open arrows indicate the ~2.2- and ~1.0-kb transcripts of PhdA, respectively. The bottom panel shows the expression pattern of cAMP receptor cAR1. (C) Sequence comparison of PhdA and CRAC (Insall et al., 1994). Asterisks indicate the sites of mutations used in this study. (D) Comparison of the PH domain of PhdA with other PH domains from *Dictyostelium*.

peaking at ~5 s, with the protein disassociating by ~12 s (Fig. 4, A and C). Moreover, when we place cells in a cAMP gradient, PhdA–GFP localizes to the leading edge (Fig. 4 B). These behaviors are similar to those of CRAC–GFP and PKB PH domain–GFP fusions (Parent et al., 1998; Meili et al., 1999). We then assessed the role of PI3Ks in these responses. Fig. 4, A and B, show that neither global stimulation nor directional stimulation (gradient of cAMP) lead to the translocation of PhdA–GFP from the cytosol to the plasma membrane in *pi3k1/2*-null cells, suggesting that the membrane localization is dependent on PI3K activity. To confirm this conclusion, we pretreated aggregation-competent wild-type cells expressing PhdA–GFP with various concentrations of LY294002 and examined the ability of cAMP to stimulate PhdA–GFP translocation. A slight delay in the response is seen with 10 μM LY294002; a concentration ≥30 μM results in complete inhibition (Fig. 4, A and C).

To examine whether the requirement of PI3K for PhdA translocation is a general property of PH domains known to translocate to the plasma membrane in response to chemoattractant signaling, we performed a similar set of experiments in wild-type cells treated with LY294002 using GFP fusions of the PH domain of PKB and CRAC (Parent et al., 1998; Meili et al., 1999). In both cases, we observed the same dose-dependent inhibition of translocation of these GFP fusion proteins as we did with PhdA (data not shown). These results suggest that PI3K is required to regulate the transient chemoattractant-mediated

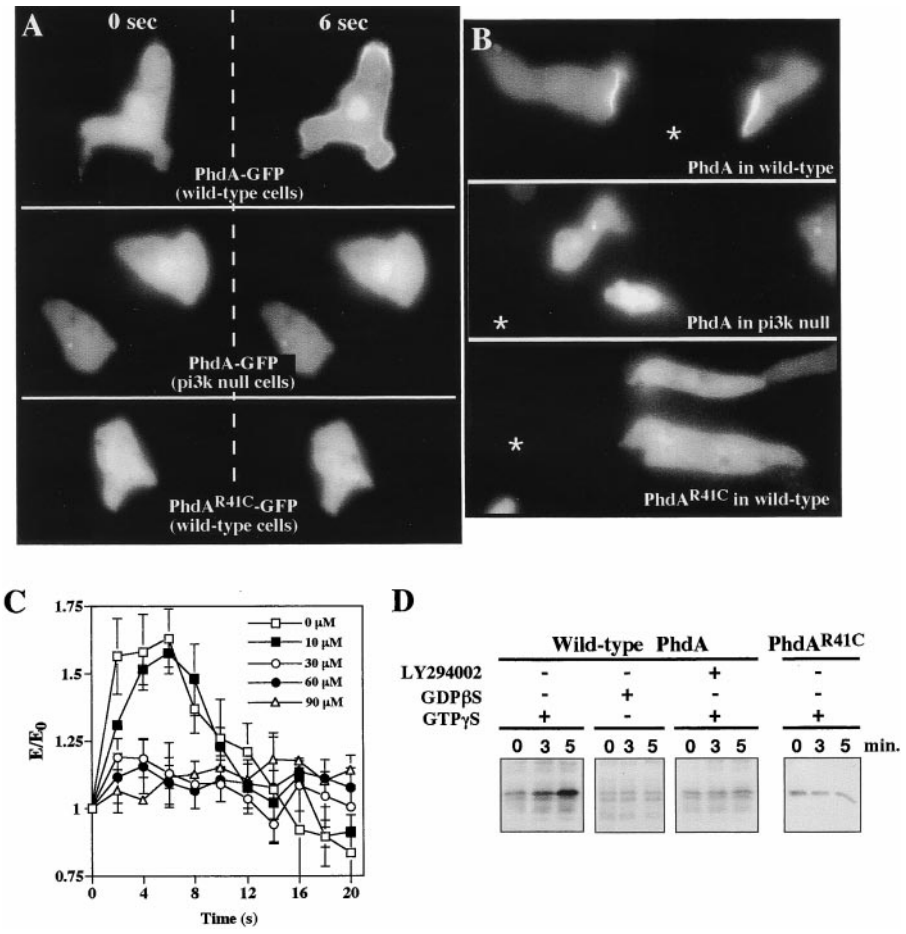

Figure 4. Translocation of PhdA–GFP in response to cAMP stimulation. (A) Global stimulation of cells by dropping cAMP solution. Wild-type cells expressing the PhdA–GFP fusion protein exhibit translocation of the protein to the cell membrane (top). In contrast, PhdA–GFP expressed in *pi3k1/2*-null cells distributes uniformly throughout the cell after stimulation with cAMP (middle). Wild-type cells expressing PhdA^{R41C}–GFP fusion protein exhibit no translocation of the protein after stimulation (bottom). (B) Accumulation of PhdA–GFP at the leading edge of migrating cells. Wild-type cells migrating toward cAMP source show a distinct localization of PhdA–GFP at the leading edge (top); *pi3k1/2*-null cells do not (middle). PhdA^{R41C}–GFP in migrating wild-type cells localizes uniformly (bottom). Asterisks indicate the position of the tip of the micropipette containing the cAMP solution. (C) Dose–response curves of LY294002 inhibition of PhdA–GFP translocation to the plasma membrane. (D) In vitro translocation of PhdA–GFP by GTPγS (as described in Materials and Methods). Membrane fractions were collected by centrifugation and PhdA–GFP was subjected to immunological detection using an anti-GFP antibody.

membrane localization of this class of PH domain–containing proteins.

To further examine the role of PI3K and other upstream pathways on PhdA translocation, we employed an in vitro translocation assay (Lilly and Devreotes, 1995; Parent et al., 1998). Wild-type cells expressing PhdA–GFP were lysed in the presence or absence of GTPγS or GDPβS and incubated. The reaction was stopped, and the membrane fraction was processed for Western blot analysis using an anti-GFP antibody. Fig. 4 D indicates that PhdA–GFP translocates to the particulate plasma membrane–containing fraction when the cells are lysed in the presence of GTPγS but not GDPβS. This GTPγS-dependent translocation is blocked when the lysates are preincubated with LY294002 in a dose-dependent fashion, indicating that the translocation is PI3K dependent (Fig. 4 D; data not shown).

It was demonstrated previously that a conserved Arg residue within PH domains is required for PI(3,4,5)P_3 binding (Fukuda et al., 1996; Salim et al., 1996; Hyvonen and Saraste, 1997; Isakoff et al., 1998). Mutation of this Arg (Arg^{25})→Cys in the Akt1 PH domain or Arg^{28}→Cys in Btk abrogates the binding of these PH domains to PI(3,4,5)P_3. Although PhdA–GFP completely restores the developmental defects of *phdA*-null cells, PhdA–GFP with an equivalent mutation (PhdA^{R41C}–GFP) expressed at comparable levels does not complement *phdA*-null cells (data not shown). Moreover, PhdA^{R41C}–GFP does not translocate to the plasma membrane or leading edge on global or directional chemoattractant stimulation (Fig. 4, A and B) nor does it bind membrane fractions from GTPγS-treated cell lysates (Fig. 4 D). These results indicate that the PH domain is integral to PhdA function and further support the conclusion that PI3Ks, presumably functioning through the formation of PI(3,4,5)P_3 and/or PI(3,4)P_2, mediate PhdA membrane translocation.

phdA-null Cells Are Defective in Chemotaxis

The small aggregate size produced by *phdA*-null cells, which is similar to that of *mek1*-null cells (Ma et al., 1997), suggests that PhdA might be required for chemotaxis. Time-lapse videomicroscopy of cells plated as a monolayer on nonnutrient agar shows that after ~3 h of starvation, wild-type cells form discernible discrete domains with aggregation centers, which act as oscillators for the initiation of waves of the chemoattractant cAMP (Fig. 5 A). These waves move outward from the center and control the inward chemotaxis of cells, leading to the formation of a multicellular organism (Siegert and Weijer, 1991) and can be "visualized" through the changes in cell shape resulting from cytoskeletal reorganizations. At ~3.5–4 h, wild-type cells start to chemotax inward, forming large discrete mounds by 6–7 h. In contrast, *phdA*-null cells display a more random pattern with multiple, smaller, and less distinct aggregation centers (Fig. 5 B). Chemotaxis is initiated at ~4 h, but instead of cells moving to a small number of discrete centers random wave patterns persist, and the cells

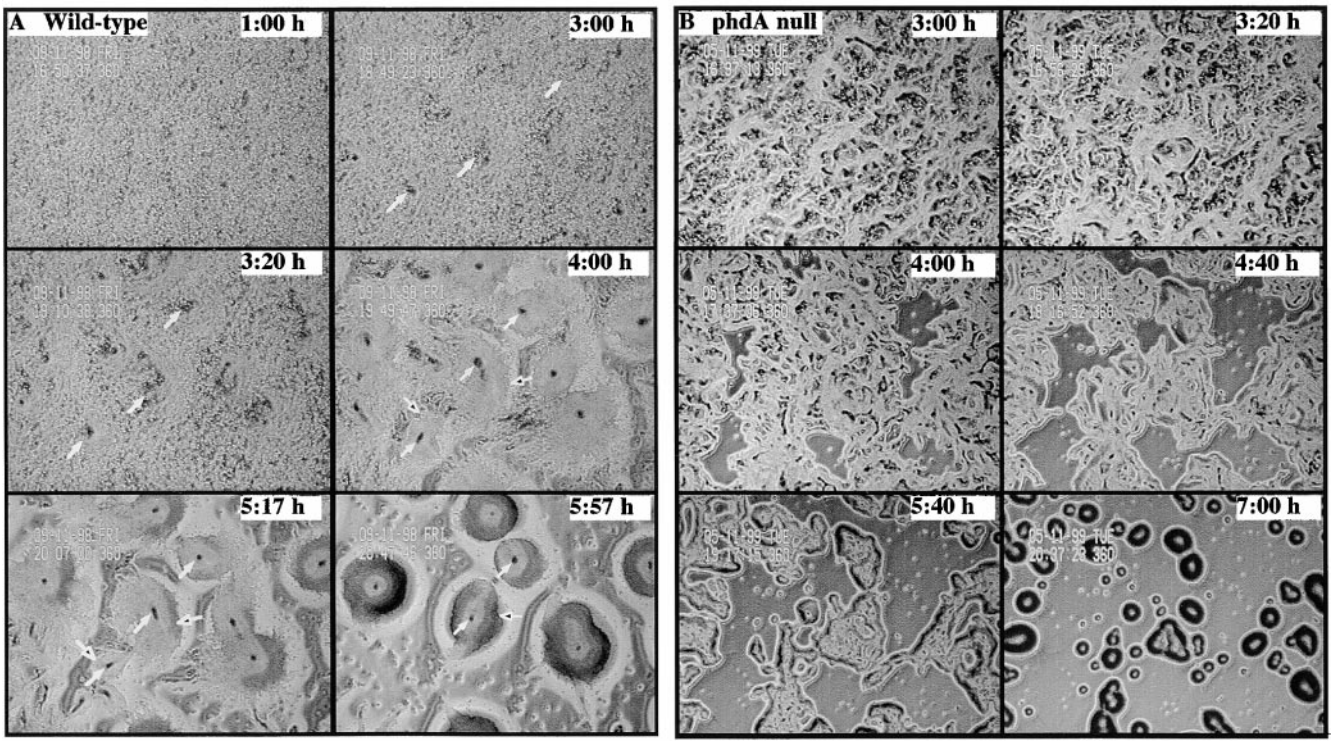

Figure 5. Time-lapse phase–contrast microscopy of wild-type and *phdA*-null cells during aggregation. Log-phase cells were washed and plated as a monolayer on nonnutrient agar plates, and aggregation was recorded as described previously (Ma et al., 1997). (A) Wild-type cells. White arrows indicate aggregation centers. Black arrows mark the outer limits of the aggregation domain. (B) *phdA*-null cells. *phdA*-null cells show a random wave pattern with multiple and less distinct aggregation centers from 4:00 to 5:40 h. Although wave patterns are observed, the cells form aberrant aggregates that break up into small distinct ones at 7:00 h.

appear to randomly coalesce into ill-formed, asymmetric aggregates (see image at 5:40 h), which eventually break up into small distinct aggregates (7:00-h image). In contrast to wild-type cells, no aggregation streams are observed.

Further analysis demonstrates that the aggregation defect observed in *phdA*-null cells is caused by a defect in chemotaxis. We find that *phdA*-null cells chemotax more slowly and make significantly more changes in direction than wild-type cells (Fig. 6, A and C, and Table I). Analysis of cell shape revealed morphological differences between *phdA*-null and wild-type cells. Wild-type cells are more elongated (polarized) than *phdA*-null cells (Table I) and have a round fairly smooth pseudopod/lamellipod at the leading edge. In contrast, the leading edge of *phdA*-null cells consists of multiple small projections or fingers that change with time (Fig. 6 B). Analysis of random motility (in the absence of a chemoattractant gradient) by DIAS revealed no significant differences between wild-type and *phdA*-null cells (data not shown), suggesting that PhdA may regulate pseudopod formation during chemotaxis.

To ensure that *phdA*-null cells are developmentally competent to respond to the cAMP signal, we examined the expression of two aggregation-stage developmental markers: the cAMP receptor cAR1 and the cell adhesion molecule contact sites A. Northern blot analysis revealed that *phdA*-null cells exhibit normal expression of both genes (Fig. 3 B; data for contact site A not shown). In addition, we measured the cAMP-mediated activation of adenylyl cyclase in *phdA*-null cells and observed that *phdA*-null and wild-type cells exhibit indistinguishable levels of adenylyl cyclase activity (data not shown), indicating the *phdA*-null cell aggregation defects are not due to an inability to relay the chemoattractant signal.

phdA-null Cells Are Defective in the Kinetics and Level of Actin Polymerization

Because of the chemotaxis phenotypes exhibited by *phdA*-null cells, we investigated whether these cells exhibit defects in F-actin polymerization. Upon global stimulation with cAMP, *phdA*-null cells exhibit kinetics of F-actin polymerization that are similar to those of wild-type cells (within the limits of this assay); however, the level of F-actin is reduced, although not to the extent observed in *pi3k1/2*-null cells (Fig. 7 A). Like *pi3k1/2*-null cells, the basal level of F-actin in unstimulated cells is reduced. As a control, we examined the kinetics and level of F-actin in *pkbA*-null cells, which were indistinguishable from those of wild-type cells (Fig. 7 A), suggesting that differences between wild-type and *phdA*-null cells are not due to any mutation in a PI3K effector.

We then used GFP-coronin to examine the spatial regulation of chemoattractant-mediated F-actin accumulation. Upon global stimulation, *phdA*-null cells exhibit a small but reproducible shift of the curve with a peak at ~7 s, compared with 5 s for wild-type cells (data not shown). When we examined the ability of *phdA*-null cells to retract an old pseudopod and form a new one when the micropipette is moved, we observed that the response was signifi-

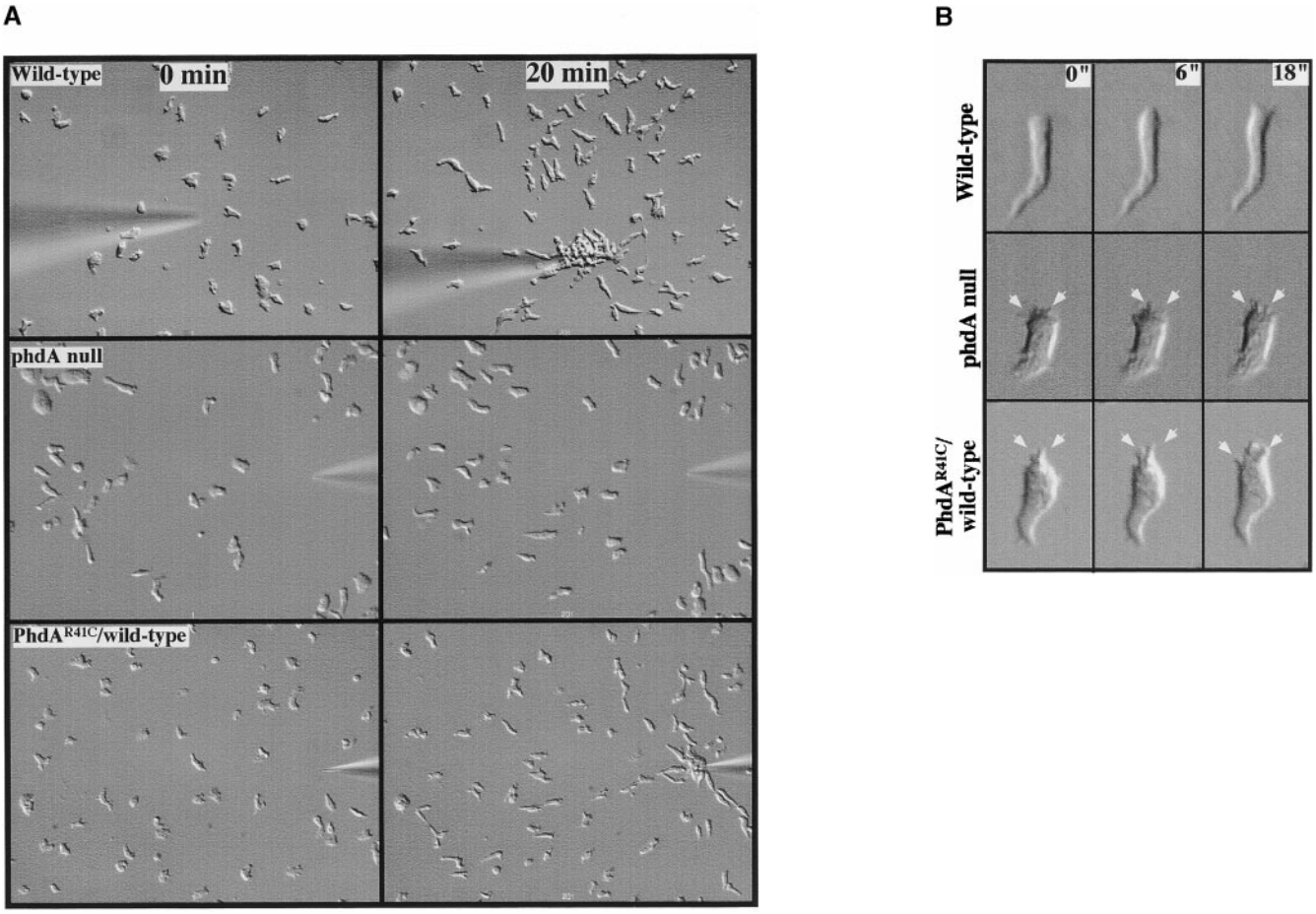
A
Wild-type
0 min
20 min
phdA null
PhdA^R41C/wild-type
B
0"
6"
18"
Wild-type
phdA null
PhdA^R41C/ wild-type
C
Wild-type (KAx-3)
phdA-
PhdA^R41C/KAx-3
PhdA/phdA-
Direction Change (deg)
Time (min)

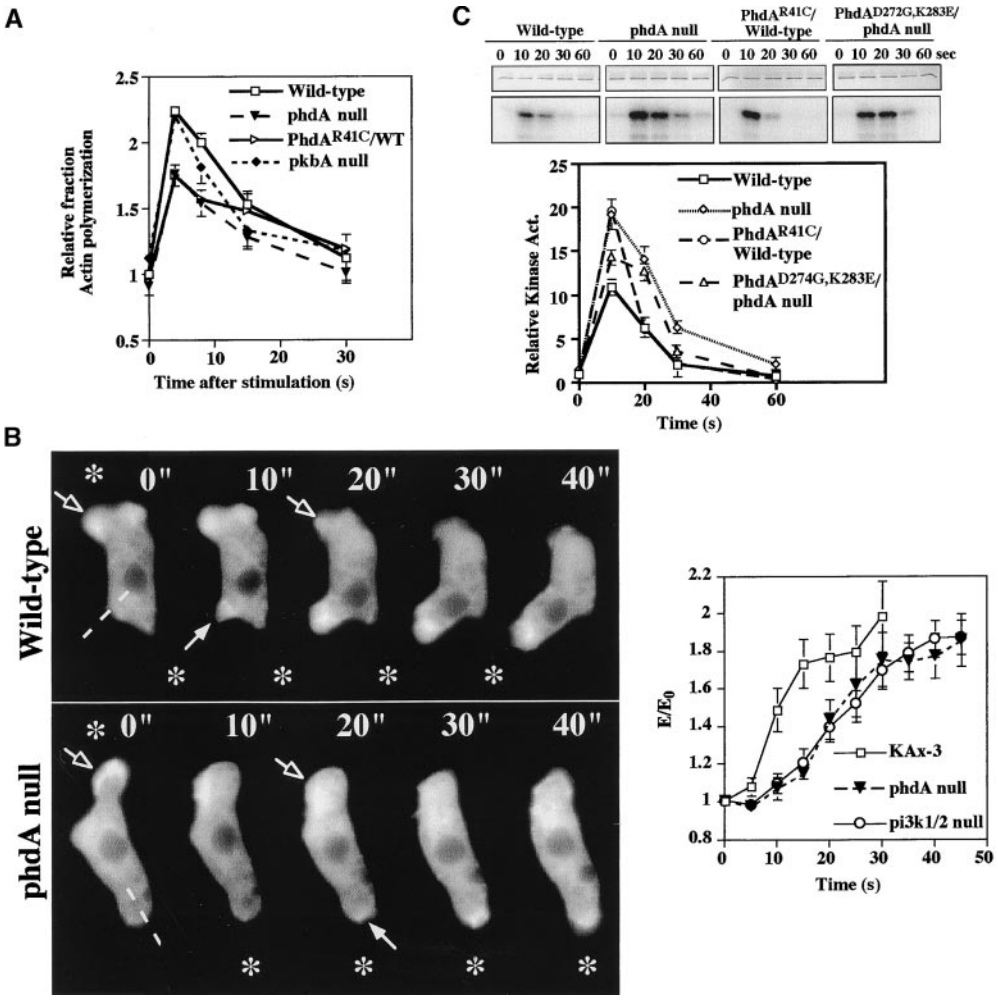

Figure 7. Regulation of F-actin in *phdA*-null cells. (A) F-actin levels in wild-type cells, *phdA*-null cells, wild-type cells expressing PhdA^{R41C}, *phdA*-null cells expressing PhdA, and *pkbA*-null cells after cAMP stimulation. See the legend to Fig. 2 for details. (B) Kinetics of GFP-coronin translocation in *phdA*-null cells (see legend to Fig. 2). The asterisks indicate the position of the micropipette containing the chemoattractant. The black arrow indicates the retracting pseudopod, and the white arrow indicates the new pseudopod. The data for wild-type and *pi3k1/2*-null cells are taken from Fig. 2. The graph represents an averaging of five cells from the same experiment. The experiment was repeated several times on the same day and three different times on different days; all experiments produced comparable results. (C) cAMP-mediated PKB kinase activity. PKB activity was tested according to Meili et al. (1999). PKB protein levels were determined in these samples using Western blot analysis (Meili et al., 1999).

cantly delayed in *phdA*-null cells, with the half-maximal response occurring at ~20 s and a delay in the initiation of the response (Fig. 7 B), similar to observations in *pi3k1/2*-null cells (Figs. 2 and 7 B). The kinetics of loss of the old pseudopod, as determined by the loss of GFP-coronin, were also significantly slower in *phdA*-null cells. This suggests that both *phdA*-null and *pi3k1/2*-null cells have a defect in the ability of cells to establish a new pseudopod and in the spatiotemporal regulation of F-actin assembly.

Figure 6. Chemotaxis of *PhdA* mutant strains to a cAMP source. (A) Chemotaxis of *phdA*-null cells to a micropipette filled with cAMP (see legend to Fig. 1; the wild-type panels are the same as those in Fig. 1 and are added as a comparison). Wild-type cells expressing PhdA^{R41C} partially phenocopy the *phdA*-null phenotype. (B) Leading edge of the *phdA*-null cell. The leading edge of a migrating wild-type cell is smooth, but the *phdA*-null cell forms multiple spike structures at the leading edge. Wild-type cells expressing PhdA^{R41C} exhibit similar projections. Arrows indicate leading edge protrusions. (C) DIAS computer analyses of *phdA* mutants (see legend to Fig. 1). *phdA*-null cells exhibit more changes of direction than wild-type cells. Wild-type cells expressing PhdA^{R41C} exhibit a reduction in elongation and movement and an increase in the change of direction as *phdA*-null cells.

PhdA Is Not Required for PKB Activation or Myosin Assembly

To examine the possible genetic interaction of PhdA with PKB, we measured the chemoattractant-mediated activation of PKB activity and PKB expression level in *phdA*-null cells. *phdA*-null cells exhibit an enhanced activation of PKB kinase activity in response to cAMP (Fig. 7 C). The kinetics of PKB activation and adaptation and PKB expression levels are similar to those of wild-type cells, suggesting that the chemotaxis defect of *phdA*-null cells is not due to a problem in the chemoattractant-mediated activation of PKB. The increased activation of PKB could be due to a change in the kinetics and/or to the extent of the localization of the subclass of PH domain that responds to the activation of PI3K; for example, the loss of PhdA might reduce competition for a limiting number of PH domain–binding sites at the leading edge, resulting in an increase in PKB activation. To examine this, we tested the kinetics of localization of CRAC-GFP, the PKB PH domain–GFP fusion, and a GFP fusion of a mutant PhdA that is able to translocate but not complement the *phdA*-null phenotype (PhdA^{D272G,E283K}–GFP, see below) expressed in *phdA*-null cells. All three GFP PH domain protein fusions exhibit the same kinetics of translocation in response to global stimulation and in a relocalization assay in which the position of the micropipette is changed within

the limits of these assays (data not shown). Our data suggest that the increased level of PKB activation in *phdA*-null cells is not due to a loss of competition of PH domains for limiting $PI(3,4,5)P_3$ and/or $PI(3,4)P_2$. Furthermore, *phdA*-null cells expressing $PhdA^{D272G,E283K}$–GFP exhibit a level of PKB activation between those of *phdA*-null and wild-type cells (Fig. 7 C). To determine if increased PKB activity results in chemotaxis defects similar to those of *phdA*-null cells, we examined chemotaxis of wild-type cells overexpressing PKB (Meili et al., 1999). These cells exhibit essentially wild-type chemotaxis (Table I), indicating that the increased PKB activation in *phdA*-null cells does not underlie the *phdA*-null chemotaxis defects. Since the chemotaxis defects of *phdA* and *pkbA*-null cells are distinct, we suggest that PhdA and PKB regulate different effector pathways downstream from PI3K.

We examined two other pathways required for chemotaxis: chemoattractant stimulation of guanylyl cyclase and myosin II assembly, which is required for cortical tension and retraction of the posterior cell body (Wessels et al., 1988). Cyclic GMP is a second messenger that regulates chemotaxis (van Haastert and Kuwayama, 1997). Guanylyl cyclase is rapidly stimulated in response to cAMP in wild-type cells, with levels of cGMP peaking at ~10 s (Mato et al., 1977). *phdA*-null cells exhibit an ~30% decrease in receptor-mediated cGMP production (data not shown). This effect alone might not cause the observed chemotaxis defect of the *phdA*-null cells. Examination of cells expressing myosin II–GFP (Moores et al., 1996) indicated a similar posterior localization of myosin II–GFP in chemotaxing wild-type and *phdA*-null cells (data not shown). Moreover, the level of assembled myosin II was the same in *phdA*-null and wild-type cells (data not shown), suggesting that PhdA does not regulate myosin II.

PhdA May Function as an Adaptor Protein

Other than the PH domain, the sequence of PhdA provides little insight into how it might function. $PhdA^{R41C}$ does not localize to the plasma membrane and does not complement the null cell. If PhdA were to function by localizing components required for chemotaxis to the leading edge, we reasoned that $PhdA^{R41C}$ might act as a dominant negative form when expressed in wild-type cells by sequestering these components in the cytosol. As shown in Fig. 6 and Table I, the expression of $PhdA^{R41C}$ in wild-type cells leads to chemotaxis defects that are similar to but less severe than those of *phdA*-null cells. This dominant interfering phenotype of $PhdA^{R41C}$ supports a model in which PhdA might function as a docking site for other proteins at the leading edge. If this were the case, point mutations in the COOH-terminal domain might abrogate PhdA function but not alter its membrane localization. We identified a PhdA mutant carrying two point mutations in the COOH-terminal domain ($PhdA^{D272G,E283K}$) resulting from PCR amplification. A $PhdA^{D272G,E283K}$–GFP fusion translocates to the plasma membrane, but neither this fusion nor $PhdA^{D272G,E283K}$ without the GFP tag complements the null phenotype, indicating that the COOH-terminal domain and a functional PH domain are essential for PhdA function (data not shown). These results are consistent with our model in which PhdA functions as a docking site for cellular proteins that must assemble at the leading edge in response to chemoattractant signals.

We expanded these studies to examine whether wild-type cells expressing $PhdA^{R41C}$ exhibit an elevated level of PKB activation similar to that seen in *phdA*-null cells. Fig. 7 C indicates that $PhdA^{R41C}$-expressing cells have an elevated PKB activation. This was not observed when $PhdA^{D272G,E283K}$ was expressed in wild-type cells (data not shown).

Discussion

PI3K Is Required for Cell Polarity, Actin Polymerization, and Proper Chemotaxis

We undertook a more detailed analysis of the role of PI3K1 and PI3K2 (Zhou et al., 1995) in regulating chemotaxis. We find that *pi3k1/2*-null cells are poorly polarized, move more slowly than wild-type cells, and make large numbers of random turns that result from the simultaneous protrusion of multiple pseudopodia from the cells. The observed cell polarity phenotypes of the *pi3k1/2*-null cells are consistent with those of cells lacking PKB, a PI3K effector that is not activated in response to the chemoattractant cAMP in *pi3k1/2*-null cells (Meili et al., 1999). In addition, we demonstrate that *pi3k1/2*-null cells are defective in regulating chemoattractant-mediated actin polymerization. All of these defects were reproduced when cAMP-responsive wild-type cells were treated with the PI3K inhibitor LY294002. As the level of F-actin polymerization is normal in *pkbA*-null cells, we suggest that the actin polymerization defect is due to a PI3K effector other than PKB. *pi3k1/2*-null cells are unable to properly spatially regulate F-actin assembly and thus to properly extend F-actin–enriched pseudopodia in the direction of the chemoattractant source, which leads to chemotaxis defects and an inability to efficiently respond to changes in the direction of the chemoattractant gradient. We obtained similar results with wild-type cells treated with LY294002, suggesting that the chemotaxis phenotypes of the *pi3k1/2*-null cells probably result from a requirement for PI3K in chemotaxis rather than a developmental defect of *pi3k1/2*-null cells that renders them less responsive to cAMP, although we cannot exclude the possibility of some pleiotrophic developmental abnormalities resulting from disruption of PI3K1 and PI3K2. We were unable to examine the phenotypes of double knockouts of PI3K1 or PI3K2 and the third *Dictyostelium* class I PI3K (PI3K3). Thus, we do not know the cellular function of PI3K3, although we expect that some of the differences between *pi3k1/2*-null cells and wild-type cells treated with LY294002 may be the result of inhibiting all three PI3Ks with the drug.

The Analysis of PhdA Defines a New Subset of Chemotaxis Pathways Regulated by PI3K

Our analysis of *phdA*-null cells provides a further understanding of the molecular mechanisms by which PI3K regulates chemotaxis. PhdA, like PKB, localizes to the leading edge of chemotaxing cells, a process that is PI3K dependent and necessary for both PhdA and PKB to function. However, the phenotypes of the *phdA* and *pkbA*-null strains indicate that the two proteins have distinct cellular

functions: *pkbA*-null cells have a severe loss of cell polarity, whereas *phdA*-null cells exhibit almost normal cell polarity but are defective in the spatiotemporal regulation of actin assembly. *phdA*-null cells normally localize myosin II in the posterior of cells, whereas myosin II assembly is abrogated in *pkbA*-null cells (Chung and Firtel, 1999; Chung et al., 2001). These studies suggest that PI3K regulates chemotaxis by controlling at least two effector pathways, one through PhdA and one through PKB.

phdA-null Cells Exhibit an Abnormal Pattern of F-Actin Assembly

The F-actin assembly defect in *phdA*-null cells is different from those defined for mutations affecting Rho family proteins. Dominant negative Rac1 blocks cell polarity, chemotaxis, and F-actin assembly in chemotaxing macrophage and *Dictyostelium* cells (Allen et al., 1998; Chung et al., 2000). Although *phdA*-null cells do not chemotax effectively, they polarize and produce a pseudopod at the leading edge in the direction of the chemoattractant source significantly better than cells in which the Rac1 GTP exchange is blocked or inhibited. We view the 30% reduction in chemoattractant-mediated F-actin polymerization in *phdA*-null cells as an indicator of the potentially more significant defect in the ability to respond to changes in the direction of the chemoattractant gradient, including localized F-actin assembly required to form a new pseudopod. Using GFP-coronin as an in vivo real time reporter of the distribution and subcellular localization of F-actin formation, we observe a significant delay in the retraction of the old pseudopod and production of a new pseudopod. We interpret these changes to result from a delay in the F-actin response, although we cannot exclude the possibility that another component of the pathway leading to coronin localization may be affected in *phdA* or *pi3k1/2*-null cells. Since a pseudopod is formed by the polymerization of F-actin at the leading edge (Weiner et al., 1999), this delay in pseudopod formation is in agreement with the delay in coronin localization and may underlie the *phdA* chemotaxis defects. Another difference between wild-type and *phdA*-null cells is that *phdA*-null cells produce a pseudopod by extending multiple finger-like projections, possibly a result of the F-actin defect. Receptor-mediated activation of adenylyl cyclase and aggregation-stage gene expression are normal, suggesting that PhdA function during aggregation is restricted to the chemotaxis pathway. The defect in F-actin polymerization and subcellular localization is more severe in *pi3k1/2*-null cells than in *phdA*-null cells. One possible explanation is that additional PI3K effectors are required for the regulation of F-actin assembly.

PhdA Lies Downstream from PI3K and May Function as an Adaptor Protein

PhdA, PKB, and CRAC all contain a PH domain and translocate to the plasma membrane in response to cAMP stimulation. We present evidence suggesting that this translocation takes place in response to the activation of PI3K and the production of $PI(3,4,5)P_3$ and/or $PI(3,4)P_2$: the translocation is absent in *pi3k1/2*-null cells; a point mutation in the PH domain ($PhdA^{R41C}$) blocks the translocation; the translocation requires the function of PI3K1 and PI3K2; and the PI3K inhibitor LY294002 blocks in vivo and GTPγS-mediated in vitro translocation. We suggest that in chemotaxing cells, PI3K is preferentially activated at the leading edge, which results in the localized response. Our experiments using a point mutation in the PhdA PH domain suggest that PhdA must translocate to the plasma membrane to function properly. Parallel studies with PKB in *Dictyostelium* carrying a similar Arg mutation in the PH domain reveal that translocation of the protein to the plasma membrane is required for PKB activation and function (Meili et al., 2000).

How does PhdA regulate the actin response? We suggest that PhdA functions as an adaptor protein required to mediate responses leading to pseudopod formation at the leading edge. This model is supported by our observation that PhdA carrying a point mutation in the PH domain, which does not translocate, functions as a dominant interfering protein in wild-type cells. Moreover, point mutations in the COOH-terminal domain abrogate PhdA function without affecting its membrane localization, indicating that this domain is required for PhdA function. We propose that the PhdA COOH-terminal domain binds signaling components, possibly those regulating actin assembly, that are required for chemotaxis and localizes them to the leading edge. Expression of $PhdA^{R41C}$ in wild-type cells would inhibit chemotaxis by binding to and sequestering in the cytosol the proposed signaling components. Expression of $PhdA^{R41C}$ in wild-type cells results in an increased PKB activation with phenotypes similar to those of *phdA*-null cells. PhdA may modulate PKB activation/adaptation, but we do not know if this is direct or indirect. Regardless, we do not think this effect of PhdA is crucial to its role in controlling chemotaxis. Since *phdA*-null cells can polymerize actin and move, albeit slowly, we suggest that these pathways are not completely abrogated in *phdA*-null cells and can function, although less efficiently, without PhdA.

Our in vitro analysis indicates involvement of the GTP-bound form of G proteins in mediating PhdA translocation, but we do not know which G proteins are required. The heterotrimeric G protein associated with the cAMP receptor ($G\alpha2/\beta\gamma$) is required for PKB activation (Meili et al., 1999), and a point mutation in the PI3K1 Ras-binding site abrogates the ability of PI3K1 to complement *pi3k1/2*-null cells with respect to activation of PKB (Meili, R., S. Funamoto, and R.A. Firtel, unpublished observations). Both Gα2 and Ras may also be required for PhdA translocation in vivo, although we cannot exclude involvement of other G proteins.

Our work is consistent with the model that the key function of PI3K is to provide binding sites ($PI[3,4,5]P_3$ and/or $PI[3,4]P_2$) for the localization of these proteins to the plasma membrane. The inability of myr-tagged proteins (PhdA and PKB), which localize uniformly along the whole plasma membrane, to complement the null phenotypes is consistent with a model in which the proteins must localize to the leading edge to properly function; the uniform distribution of membrane-localized PhdA may impair chemotaxis by not localizing the response to the leading edge. The observations that mammalian PKB is activated in response to chemoattractants, a mammalian PKB PH domain–GFP fusion localizes to the leading edge

in chemotaxing neutrophils, and mammalian PKB is not activated in *pi3kγ*-null cells (see Introduction) suggest that the role of PKB in *Dictyostelium* chemotaxis may be conserved in mammalian cells. Although PhdA does not have a direct homologue in other systems, the requirement for multiple, coordinated, localized effector responses, including actin polymerization and coronin function, at the leading edge in eukaryotic chemotaxing cells suggests that other PH domain–containing proteins with similar functions exist in metazoans, and PI3K provides binding sites for the localization and activation of these proteins.

We thank Carole Parent for graciously performing the adenylyl cyclase assays and allowing us to use these data, N. Iranfar and W. Loomis for the PhdA restriction enzyme–mediated integration mutant, Firtel laboratory members for helpful suggestions, and Jennifer Roth for critical reading of the manuscript.

S. Funamoto was supported in part by a Japanese Society for the Promotion of Science Research Fellowship for Young Scientists. This work was supported by U.S. Public Health Service grants to R.A. Firtel.

Submitted: 29 November 2000
Revised: 20 March 2001
Accepted: 29 March 2001

References

Allen, W.E., D. Zicha, A.J. Ridley, and G.E. Jones. 1998. A role for Cdc42 in macrophage chemotaxis. *J. Cell Biol.* 141:1147–1157.

Andjelkovic, M., D.R. Alessi, R. Meier, A. Fernandez, N.J. Lamb, M. Frech, P. Cron, P. Cohen, J.M. Lucocq, and B.A. Hemmings. 1997. Role of translocation in the activation and function of protein kinase B. *J. Biol. Chem.* 272: 31515–31524.

Brunet, A., A. Bonni, M.J. Zigmond, M.Z. Lin, P. Juo, L.S. Hu, M.J. Anderson, K.C. Arden, J. Blenis, and M.E. Greenberg. 1999. Akt promotes cell survival by phosphorylating and inhibiting a forkhead transcription factor. *Cell*. 96: 857–868.

Buczynski, G., B. Grove, A. Nomura, M. Kleve, J. Bush, R.A. Firtel, and J. Cardelli. 1997. Inactivation of two *Dictyostelium discoideum* genes, DdPIK1 and DdPIK2, encoding proteins related to mammalian phosphatidylinositide 3-kinases, results in defects in endocytosis, lysosome to postlysosome transport, and actin cytoskeleton organization. *J. Cell Biol.* 136:1271–1286.

Carboni, J.M., and J.S. Condeelis. 1985. Ligand-induced changes in the location of actin, myosin, 95K (alpha-actinin), and 120K protein in amebae of *Dictyostelium discoideum*. *J. Cell Biol.* 100:1884–1893.

Cardone, M.H., N. Roy, H.R. Stennicke, G.S. Salvesen, T.F. Franke, E. Stanbridge, S. Frisch, and J.C. Reed. 1998. Regulation of cell death protease caspase-9 by phosphorylation. *Science*. 282:1318–1321.

Chung, C., S. Lee, C. Briscoe, C. Ellsworth, and R.A. Firtel. 2000. Role of Rac in controlling the actin cytoskeleton and chemotaxis in motile cells. *Proc. Natl. Acad. Sci. USA*. 97:5225–5230.

Chung, C.Y., and R.A. Firtel. 1999. PAKa, a putative PAK family member, is required for cytokinesis and the regulation of the cytoskeleton in *Dictyostelium discoideum* cells during chemotaxis. *J. Cell Biol.* 147:559–575.

Chung, C.Y., G. Potikyan, and R.A. Firtel. 2001. Control of cell polarity and chemotaxis by Akt/PKB and PI3 kinase through the regulation of PAKa. *Mol. Cell.* In press.

Condeelis, J., and A.L. Hall. 1991. Measurement of actin polymerization and cross-linking in agonist-stimulated cells. *Methods Enzymol.* 196:486–496.

Cross, D., D. Alessi, P. Cohen, M. Anjelkovich, and B. Hemmings. 1995. Inhibition of glycogen synthase kinase-3 by insulin mediated by protein kinase B. *Nature*. 378:785–789.

Datta, S.R., H. Dudek, X. Tao, S. Masters, H. Fu, Y. Gotoh, and M.E. Greenberg. 1997. Akt phosphorylation of BAD couples survival signals to the cell-intrinsic death machinery. *Cell*. 91:231–241.

Dunzendorfer, S., C. Meierhofer, and C.J. Wiedermann. 1998. Signalling in neuropeptide-induced migration of human eosinophils. *J. Leukoc. Biol.* 64: 828–834.

Firtel, R.A., and C.Y. Chung. 2000. The molecular genetics of chemotaxis: sensing and responding to chemoattractant gradients. *BioEssays*. 22:603–615.

Fukuda, M., T. Kojima, H. Kabayama, and K. Mikoshiba. 1996. Mutation of the pleckstrin homology domain of Bruton's tyrosine kinase in immunodeficiency impaired inositol 1,3,4,5-tetrakisphosphate binding capacity. *J. Biol. Chem*. 271:30303–30306.

Gerisch, G., R. Albrecht, C. Heizer, S. Hodgkinson, and M. Maniak. 1995. Chemoattractant-controlled accumulation of coronin at the leading edge of *Dictyostelium* cells monitored using green fluorescent protein-coronin fusion protein. *Curr. Biol.* 5:1280–1285.

Gold, M.R., M.P. Scheid, L. Santos, M. Dang-Lawson, R.A. Roth, L. Matsuuchi, V. Duronio, and D.L. Krebs. 1999. The B cell antigen receptor activates the Akt (protein kinase B)/glycogen synthase kinase-3 signaling pathway via phosphatidylinositol 3-kinase. *J. Immunol*. 163:1894–1905.

Hirsch, E., V.L. Katanaev, C. Garlanda, O. Azzolino, L. Pirola, L. Silengo, S. Sozzani, A. Mantovani, F. Altruda, and M.P. Wymann. 2000. Central role for G protein-coupled phosphoinositide 3-kinase gamma in inflammation. *Science*. 287:1049–1053.

Hyvonen, M., and M. Saraste. 1997. Structure of the PH domain and Btk motif from Bruton's tyrosine kinase: molecular explanations for X-linked agammaglobulinaemia. *EMBO J*. 16:3396–3404.

Insall, R., A. Kuspa, P.J. Lilly, G. Shaulsky, L.R. Levin, W.F. Loomis, and P. Devreotes. 1994. CRAC, a cytosolic protein containing a pleckstrin homology domain, is required for receptor and G protein–mediated activation of adenylyl cyclase in *Dictyostelium*. *J. Cell Biol.* 126:1537–1545.

Isakoff, S.J., T. Cardozo, J. Andreev, Z. Li, K.M. Ferguson, R. Abagyan, M.A. Lemmon, A. Aronheim, and E.Y. Skolnik. 1998. Identification and analysis of PH domain-containing targets of phosphatidylinositol 3-kinase using a novel in vivo assay in yeast. *EMBO J*. 17:5374–5387.

Kennedy, S.G., E.S. Kandel, T.K. Cross, and N. Hay. 1999. Akt/Protein kinase B inhibits cell death by preventing the release of cytochrome c from mitochondria. *Mol. Cell. Biol*. 19:5800–5810.

Leevers, S.J., B. Vanhaesebroeck, and M.D. Waterfield. 1999. Signalling through phosphoinositide 3-kinases: the lipids take centre stage. *Curr. Opin. Cell Biol.* 11:219–225.

Li, Z., H. Jiang, W. Xie, Z. Zhang, A.V. Smrcka, and D. Wu. 2000. Roles of PLC-beta2 and -beta3 and PI3Kgamma in chemoattractant-mediated signal transduction. *Science.* 287:1046–1049.

Lilly, P.J., and P.N. Devreotes. 1995. Chemoattractant and GTPγS-mediated stimulation of adenylyl cyclase in *Dictyostelium* requires translocation of CRAC to membranes. *J. Cell Biol.* 129:1659–1665.

Ma, H., M. Gamper, C. Parent, and R.A. Firtel. 1997. The *Dictyostelium* MAP kinase kinase DdMEK1 regulates chemotaxis and is essential for chemoattractant-mediated activation of guanylyl cyclase. *EMBO J.* 16:4317–4332.

Mato, J.M., F.A. Krens, P.J.M. van Haastert, and T.M. Konijn. 1977. 3′:5′-cyclic AMP-dependent 3′:5′-cyclic GMP accumulation in *Dictyostelium discoideum*. *Proc. Natl. Acad. Sci. USA*. 74:2348–2351.

Meili, R., C. Ellsworth, S. Lee, T.B. Reddy, H. Ma, and R.A. Firtel. 1999. Chemoattractant-mediated transient activation and membrane localization of Akt/PKB is required for efficient chemotaxis to cAMP in *Dictyostelium*. *EMBO J*. 18:2092–2105.

Meili, R., C. Ellsworth, and R.A. Firtel. 2000. A novel Akt/PKB-related kinase is essential for morphogenesis in *Dictyostelium*. *Curr. Biol.* 10:708–717.

Moniakis, J., S. Funamoto, M. Fukuzawa, J. Meisenhelder, T. Araki, T. Abe, R. Meili, T. Hunter, J. Williams, and R. Firtel. 2001. An SH2-domain-containing kinase is a negative regulator of the phosphatidylinositol-3 kinase pathway. *Genes Dev*. 15:687–698.

Moores, S.L., J.H. Sabry, and J.A. Spudich. 1996. Myosin dynamics in live *Dictyostelium* cells. *Proc. Natl. Acad. Sci. USA*. 93:443–446.

Osada, M., T. Tolkacheva, W. Li, T.O. Chan, P.N. Tsichlis, R. Saez, A.C. Kimmelman, and A.M. Chan. 1999. Differential roles of Akt, Rac, and Ral in R-Ras-mediated cellular transformation, adhesion, and survival. *Mol. Cell. Biol*. 19:6333–6344.

Paradis, S., and G. Ruvkun. 1998. *Caenorhabditis elegans* Akt/PKB transduces insulin receptor-like signals from AGE-1 PI3 kinase to the DAF-16 transcription factor. *Genes Dev*. 12:2488–2498.

Parent, C.A., and P.N. Devreotes. 1995. Isolation of inactive and G protein-resistant adenylyl cyclase mutants using random mutagenesis. *J. Biol. Chem.* 270:22693–22696.

Parent, C.A., and P.N. Devreotes. 1999. A cell's sense of direction. *Science*. 284: 765–770.

Parent, C.A., B.J. Blacklock, W.M. Froehlich, D.B. Murphy, and P.N. Devreotes. 1998. G protein signaling events are activated at the leading edge of chemotactic cells. *Cell*. 95:81–91.

Rameh, L.E., and L.C. Cantley. 1999. The role of phosphoinositide 3-kinase lipid products in cell function. *J. Biol. Chem*. 274:8347–8350.

Rickert, P., O. Weiner, F. Wang, H. Bourne, and G. Servant. 2000. Leukocytes navigate by compass: roles of PI3K-gamma and its lipid products. *Trends Cell Biol.* 10:466–473.

Salim, K., M.J. Bottomley, E. Querfurth, M.J. Zvelebil, I. Gout, R. Scaife, R.L. Margolis, R. Gigg, C.I. Smith, P.C. Driscoll, M.D. Waterfield, and G. Panayotou. 1996. Distinct specificity in the recognition of phosphoinositides by the pleckstrin homology domains of dynamin and Bruton's tyrosine kinase. *EMBO J*. 15:6241–6250.

Sasaki, T., J. Irie-Sasaki, R.G. Jones, A.J. Oliveira-dos-Santos, W.L. Stanford, B. Bolon, A. Wakeham, A. Itie, D. Bouchard, I. Kozieradzki, et al. 2000. Function of PI3Kgamma in thymocyte development, T cell activation, and neutrophil migration. *Science.* 287:1040–1046.

Servant, G., O.D. Weiner, P. Herzmark, T. Balla, J.W. Sedat, and H.R. Bourne. 2000. Polarization of chemoattractant receptor signaling during neutrophil chemotaxis. *Science*. 287:1037–1040.

Siegert, F., and C.J. Weijer. 1991. Analysis of optical density wave propagation and cell movement in the cellular slime mold *Dictyostelium discoideum*. *Physica D*. 49:224–232.

Soll, D., and E. Voss. 1998. Two- and three-dimensional computer systems for

analyzing how animal cells crawl. *In* Motion Analysis of Living Cells. D. Soll and D. Wessels, editors. Wiley-Liss, New York. 25–52.

Tang, E.D., G. Nuñez, F.G. Barr, and K.L. Guan. 1999. Negative regulation of the forkhead transcription factor FKHR by Akt. *J. Biol. Chem*. 274:16741–16746.

Tilton, B., M. Andjelkovic, S.A. Didichenko, B.A. Hemmings, and M. Thelen. 1997. G-protein-coupled receptors and Fcgamma-receptors mediate activation of Akt/protein kinase B in human phagocytes. *J. Biol. Chem*. 272: 28096–28101.

van Haastert, P.J.M., and H. Kuwayama. 1997. cGMP as second messenger during *Dictyostelium* chemotaxis. *FEBS Lett.* 410:25–28.

Vanhaesebroeck, B., and M.D. Waterfield. 1999. Signaling by distinct classes of phosphoinositide 3-kinases. *Exp. Cell Res.* 253:239–254.

Vanhaesbroeck, B., S. Leevers, G. Panayotou, and M. Waterfield. 1997. Phosphoinositide 3-kinases: a conserved family of signal transducers. *Trends Biochem. Sci.* 22:267–272.

Vanhaesebroeck, B., G.E. Jones, W.E. Allen, D. Zicha, R. Hooshmand-Rad, C. Sawyer, C. Wells, M.D. Waterfield, and A.J. Ridley. 1999. Distinct PI(3)Ks mediate mitogenic signalling and cell migration in macrophages. *Nat. Cell Biol.* 1:69–71.

Varnum, B., and D.R. Soll. 1981. Chemoresponsiveness to cAMP and folic acid during growth, development, and dedifferentiation in *Dictyostelium discoideum*. *Differentiation*. 18:151–160.

Weiner, O.D., G. Servant, M.D. Welch, T.J. Mitchison, J.W. Sedat, and H.R. Bourne. 1999. Spatial control of actin polymerization during neutrophil chemotaxis. *Nat. Cell Biol*. 1:75–81.

Weinkove, D., T.P. Neufeld, T. Twardzik, M.D. Waterfield, and S.J. Leevers. 1999. Regulation of imaginal disc cell size, cell number and organ size by *Drosophila* class I(A) phosphoinositide 3-kinase and its adaptor. *Curr. Biol.* 9:1019–1029.

Wessels, D., D.R. Soll, D. Knecht, W.F. Loomis, A. De Lozanne, and J. Spudich. 1988. Cell motility and chemotaxis in *Dictyostelium* amebae lacking myosin heavy chain. *Dev. Biol.* 128:164–177.

Zhou, K., S. Pandol, G. Bokoch, and A.E. Traynor-Kaplan. 1998. Disruption of *Dictyostelium* PI3K genes reduces [^{32}P]phosphatidylinositol 3,4 bisphosphate and [^{32}P]phosphatidylinositol trisphosphate levels, alters F-actin distribution and impairs pinocytosis. *J. Cell Sci*. 111:283–294.

Zhou, K.M., K. Takegawa, S.D. Emr, and R.A. Firtel. 1995. A phosphatidylinositol (PI) kinase gene family in *Dictyostelium discoideum*: biological roles of putative mammalian p110 and yeast Vps34p PI 3-kinase homologs during growth and development. *Mol. Cell. Biol.* 15:5645–5656.